# INRIA

# Joint Estimation and Smoothing of Clinical DT-MRI with a Log-Euclidean Metric.

Pierre Fillard — Vincent Arsigny — Xavier Pennec — Nicholas Ayache

## N° 5607

June 2005

Thème BIO

*R apport de recherche*

# Joint Estimation and Smoothing of Clinical DT-MRI with a Log-Euclidean Metric.

Pierre Fillard , Vincent Arsigny , Xavier Pennec , Nicholas Ayache

**Abstract:**    Diffusion tensor MRI is an imaging modality that is gaining importance in clinical applications. However, in a clinical environment, data has to be acquired rapidly at the detriment of the image quality. We propose a new variational framework that specifically targets low quality DT-MRI. The hypothesis of an additive Gaussian noise on the images leads us to estimate the tensor field directly on the image intensities.  To further reduce the influence of the noise, we optimally exploit the spatial correlation by adding to the estimation an anisotropic regularization term. This criterion is easily optimized thanks to the use of the recently introduced Log-Euclidean metrics. Results on real clinical data show promising improvements of fiber tracking in the brain and we present the first successful attempt, up to our knowledge, to reconstruct the spinal cord.

**Key-words:**    tensors, DT-MRI, DTI, estimation, regularization, fiber tracking, Log-Euclidean, Riemannian geometry

# Estimation et Regularisation jointes d'IRM de Diffusion Clinique avec une Métrique Log-Euclidienne.

**Résumé :** L'IRM du tenseur de diffusion (DT-MRI) est une modalité d'image qui prend de plus en plus d'importance dans les applications cliniques. Cependant, dans un environnement clinique, les données doivent être acquises rapidement, souvent au détriment de la qualité des images. Nous proposons un nouveau cadre variationnel qui s'adresse spécifiquement aux IRM de diffusion bruitées. L'hypothèse d'un bruit gaussien additif sur les images nous conduit à estimer le champ de tenseurs directement à partir des intensités des images. Afin d'encore plus réduire l'influence du bruit, nous exploitons de manière optimale la corrélation spatiale en ajoutant à l'estimation un terme de régularisation anisotrope. Ce critère est facilement optimisé grâce à l'utilisation des métriques Log-Eulidienne introduites récemment. Les résultats sur des données cliniques montrent des améliorations prometteuses du suivi de fibres dans le cerveau et nous présentons la première tempative réussie, à notre connaissance, de reconstruction du faisceau de fibres de la moëlle épinière.

**Mots-clés :** tenseurs, DT-MRI, DTI, estimation, régularisation, suivi de fibres, log-euclidien, géométrie riemannienne

# Contents

# 1   Introduction

Diffusion tensor MRI (DT-MRI or DTI) [1] is a unique tool to assess in vivo oriented structures within tissues via the measure of water diffusion. However, using such an imaging modality in a clinical environment is difficult. Indeed, data must be acquired rapidly due to pathologies that often prevent the patient to stay in the same position for too long. This results in acquisitions with a limited number of encoding gradients and low signal-to-noise ratios. The estimation of the diffusion tensor field from diffusion weighted images (DWI) is noise-sensitive and consequently clinical DTI are very often not suitable for post processing, like fiber tracking. For these reasons, there has been a growing interest in the regularization of tensor images. In the following we quickly summarize the state of the art in diffusion tensor estimation and regularization.

## 1.1   Usual Tensor Field Estimation

The Stejskal-Tanner diffusion equation [1] relates the diffusion tensor $D$ to each DWI with $S_i = S_0 \exp(-b g_i^T D g_i)$, where $S_i$ is the original DWI corresponding to the encoding gradient $g_i$, $S_0$ an image with a null gradient, and $b$ the diffusion factor. To get a linear system, one usually takes the logarithm [2, 3] of the DWI, which implies the assumption of a Gaussian noise on the log of the images: $\log(S_i) = \log(S_0) - b g_i^T D g_i + N(0, \sigma)$, where $N(0, \sigma)$ is a centered Gaussian noise of variance $\sigma$. Although the noise in the MR images is known to be Rician distributed, it can be well approximated by a Gaussian distribution within the brain. Moreover, when the signal to noise ratio (SNR) is high, one can also show that the noise on the image logarithms is Gaussian distributed [4], which justifies the linearization of the diffusion equation. Finally, solving the linearized system in a least square sense leads to the minimization of a quadratic criterion with algebraic methods.

However, when working with clinical MRI, SNR is very low and the number of encoding gradients is generally limited to 6. In that case, Wang et al. argue that it is better to consider the noise to be additive on the image intensities and not on their logarithms. Then, the measured images should rather be modeled as: $\hat{S}_i = S_i + N(0, \sigma)$. The estimation criterion proposed by Wang et al. in [5] is well suited for this last model of noise. They parameterize a tensor by its Cholesky factor for the resolution, which only insures the positivity of the result and not the definiteness. We will see in Sec. 1.3 that this is actually not sufficient for our purpose.

## 1.2   Regularization of Tensor Images

For the ultimate application targeted in this paper, i.e. fiber reconstruction, the diffusion tensor field needs to be regularized without blurring the transitions between distinct fiber tracts, which delimit anatomical and functional brain regions. A first idea consists in smoothing independently each DWI. This results in a smoother tensor field but it also blurs the transitions between homogeneous regions, as this information is not accessible by taking each DWI individually. For instance, in brain DTI, only the combination of all the images

reveals the complex neural structure of the white matter. Consequently, one would like to perform an anisotropic regularization of the tensor field itself. Some regularization methods have been proposed: for instance, [6] regularizes the principal eigenvector (associated to the largest eigenvalue), while [7] uses the spectral decomposition of tensors to independently regularize their eigenvectors and eigenvalues. More recently, [5] prefers to smooth the Cholesky factors of tensors. The two former methods rely on the spectral decomposition of tensors: smoothing the major eigenvector induces a dramatical loss of information and there is also an uncertainty of the spectral decomposition in regions with flat tensors, and discontinuity problems arise when smoothing the field of orthogonal matrices as the spectral decomposition is not unique. Interestingly, the last approach has the advantage to smoothly but not uniquely parameterize the space of tensors by the vector space of lower triangular matrices, where computations can be done easily. This has to be compared to the recently proposed Riemannian metrics for tensors, which also turn the tensor space into a vector space, as in [8] and [9]. This comparison and the choice of the tool for solving our problem are discussed in the following section.

## 1.3 Tools for Tensor Computing

Tensor computing is arduous as the standard Euclidean calculus suffers from severe limitations. While convex operations are stable on the tensor space (e.g. the mean of a set of tensors is a tensor), one can quickly reach the boundaries of the space with complex operations (like partial differential equation (PDE) solving) and null or negative eigenvalues may appear. To overcome this limitation, [5] proposed to parameterize a tensor $\Sigma$ by its Cholesky factor. A Cholesky factorization of $\Sigma$ is given by: $\Sigma = LL^T$, where $L$ is a lower triangular matrix. Let us consider the singular value decomposition (SVD) of $L$: there exist $U$ and $V$ orthogonal matrices and $D$ a positive diagonal matrix such that $L = UDV^T$. Consequently, $\Sigma = LL^T = UD^2U^T$, which proves that $\Sigma$ will remain positive when working on its Cholesky factor. However, the definiteness is not insured (null eigenvalues are possible). The authors argue that forbidding negative eigenvalues is sufficient because we cannot numerically distinguish very small eigenvalues from null ones. Thus, forbidding explicitly null eigenvalues has no practical justification.

While we agree that very small eigenvalues are not distinguishable from null ones, we believe that both are very unlikely to exist from a physical point of view, and should be as far as possible from any reference tensor. In other words, a tensor with very small eigenvalues has a very low probability to appear, as well as a tensor with very large eigenvalues. Both of them must be numerically nearly impossible to reach. In general, this is a consequence of the structure of the space we are working on. Let us illustrate this with the following example. A tensor is replaced by its Cholesky factor $L$: $\Sigma = LL^T$. The distance derived from the $L_2$ norm between two tensors is written as: $\text{dist}^2(\Sigma_1, \Sigma_2) = \|L_1 - L_2\|_2^2$. The

distance between $\Sigma$ and $\lambda\Sigma$ is given by:

$$
\begin{aligned}
\text{dist}^2\left(\Sigma, \lambda\Sigma\right) &= \|L - \sqrt{\lambda}L\|^2 \\
&= (1 - \sqrt{\lambda})^2 \|L\|^2 \\
&= (1 - \sqrt{\lambda})^2 \text{Tr}(LL^T) \\
&= (1 - \sqrt{\lambda})^2 \text{Tr}(\Sigma)
\end{aligned}
$$

If $\Sigma = I_d$ (identity matrix), we find that $\text{dist}(\Sigma, 0\Sigma) = 3$ and $\text{dist}(\Sigma, 4\Sigma) = 3$. This shows that the null matrix ($\lambda = 0$) is at the same distance to $\Sigma$ than the tensor $4\Sigma$. In other words, a "null" diffusion can be reached in a finite time, and it takes the same time to reach a null diffusion than a 4 times larger diffusion. This is an improvement over the Euclidean calculus, where the null matrix and the tensor $2\Sigma$ are equidistant to $\Sigma$, but it still does not reject null and very small tensors far from any real diffusion tensor.

To emphasize the importance of the structure given to a space, we found interesting to see how a tensor behaves when the space is endowed with different structures. Basically, we simulate a PDE resolution with a simple gradient descent, i.e. in the Euclidean case one simply computes the tensors: $\Sigma_e = \Sigma - tW$, where $t \in [0, 2]$, $\Sigma = ((4, 0, 0), (0, 1, 0), (0, 0, 1))$ and $W = ((2, 0, 0), (0, 1, 0), (0, 0, 1))$. and in the second case, we compute $L_e = L - tW$, where $L$ is the Cholesky factor of $\Sigma$. $W$ could represent the gradient of a criterion we want to minimize. Results of the two extrapolation are displayed in Fig. 1. In the Euclidean case, as expected, one quickly reaches the boundaries and values that are not displayed are actually non-positive tensors. The Cholesky case is algorithmically much better posed as non-positive matrices do not appear. However, we still reach zero eigenvalues, i.e. the null matrix appears, and values beyond it are the mirrored versions of the first ones. This means that during a gradient descent, the null matrix can easily be reached. Moreover, one may question the physical meaning of the mirrored values obtained beyond the null matrix. In the Log-Euclidean case (see Sec. 2 for more details), the null matrix is never reached and all tensors are by nature positive definite. This exemplifies the need to endow the tensor space with a structure that strictly forbids the null matrix.

The recently proposed Riemannian metrics offer a solution to this constraint: In [10, 11, 12, 8] an affine-invariant Riemannian metric is proposed and the tensor space is replaced by a regular manifold where matrices with null and negative eigenvalues are at an infinite distance of any tensor. However, computations with this metric are time-consuming since they extensively use the matrix exponential, logarithm, square root and inverse. A novel family of Riemannian metrics, called Log-Euclidean and detailed in [9], combine the properties of their affine-invariant counterpart with a computational cost similar to the Euclidean case. Their properties are investigated in Sec. 2.

In summary, to address the problem of estimation of noisy clinical DTI, we rely on a similar formulation proposed by Wang et al. in [5], which combines an estimation criterion
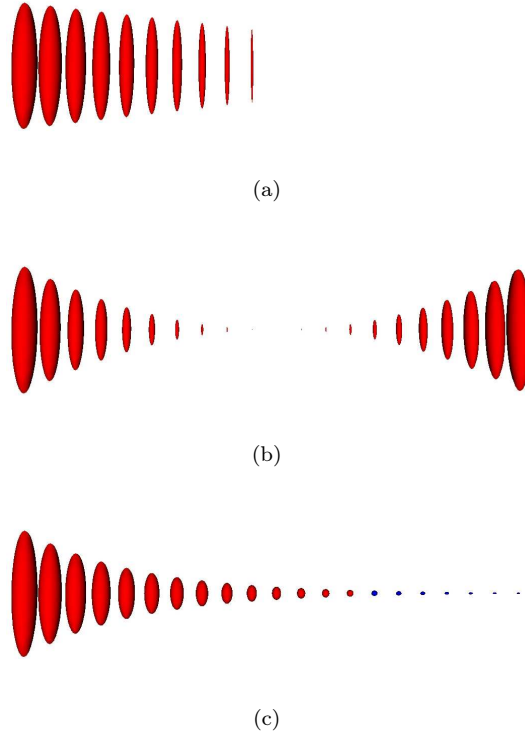
(a)

(b)

(c)

Figure 1: **Tensor evolution by simulating a gradient descent. (a):** The Euclidean case. Half of the tensors are not positive definite and thus are not displayed. **(b):** The Cholesky case: the null matrix is reached (exact middle value) and values beyond are the mirrored versions of the previous ones. **(c):** The Log-Euclidean case: all tensors are positive definite, and the null tensor is not reached as it is at an infinite distance.

on the image intensities with an anisotropic regularization term. However, to solve the problem, we propose to endow the tensor space with a Log-Euclidean Riemannian structure, which has the advantage to be not only algorithmically well sound but also physically, which is not the case when parameterizing tensors with their Cholesky factors. The rest of the paper is organized as follows. In Sec. 2, the theory and properties of Log-Euclidean metrics are presented. In Sec. 3, we detail the variational method of the joint estimation and smoothing of DTI. In Sec. 4, we present very promising results on a brain dataset, and the first successful reconstruction of a spinal cord tract.

## 2   Log-Euclidean Metrics for Tensors

In this section, we summarize the main theoretical results obtained in [9], where the theory of Log-Euclidean metrics is detailed.

**Existence and Uniqueness of the Logarithm**   To a tensor $S$ is associated a unique *logarithm $L$* which is *symmetric*. It verifies $S = \exp(L)$ where exp is the matrix exponential. To each symmetric matrix is associated by the exponential a tensor. In an orthonormal basis in which $S$ is diagonal, $L$ is obtained by transforming the eigenvalues of $S$ into their scalar logarithm.

**A Vector Space Structure on Tensors**   Since their is a one-to-one mapping between the tensor space, denoted $Sym_\star^+(n)$ and the space of symmetric matrices $Sym(n)$, one can give $Sym_\star^+(n)$ a *vector space structure* by transporting the addition $+$ and the scalar multiplication . on $Sym_\star^+(n)$ with the exponential.

This defines on $Sym_\star^+(n)$ the *logarithmic multiplication* $\odot$ and the *logarithmic scalar multiplication* $\circledast$, given by:

$$\begin{cases} S_1 \odot S_2 := \exp\left(\log(S_1) + \log(S_2)\right) \\ \lambda \circledast S := \exp\left(\lambda.\log(S)\right) = S^\lambda. \end{cases} \tag{1}$$

The logarithmic multiplication is *commutative* and coincides with the matrix multiplication whenever the two tensors $S_1$ and $S_2$ commute in the matrix sense.

With $\odot$ and $\circledast$, the tensor space has by construction a *vector space structure*. One should note that this is *not* the usual vector space structure derived from the addition and scalar multiplication on square matrices. With the latter structure, the tensor space is *not* a vector space, whereas with this new structure it *is* a vector space. The notion of vector space depends on the structure one considers, and not only on the space itself. Let us go back now to the example of the gradient descent simulation of Sec. 1.3. The Log-Euclidean formulation is: $\Sigma_e = \exp(\log(\Sigma) + tW)$. Result of the evolution is shown in Fig. 1 c: all tensors remain positive definite and the null matrix cannot be reached.

**Log-Euclidean Metrics**   When one considers only the multiplication $\odot$ on the tensor space, one has a *Lie group* structure, i.e. a space which is both a hypersurface and a group in which algebraic operations are *smooth mappings*. This viewpoint is important, because the theory of Riemannian metrics can be applied to Lie groups to define metrics, i.e. distances, in a framework where usual analysis and statistical tools can be generalized (see [13]).

Among Riemannian metrics in Lie groups, the most convenient in practice, when they exist, are *biinvariant metrics*, i.e. distances that are invariant by multiplication and inversion. For the tensor Lie group, biinvariant metrics exist and are particularly simple. We have named such metrics *Log-Euclidean* metrics, since they correspond to Euclidean metrics in the logarithmic domain. From a Euclidean norm $\|.\|$ on $Sym(n)$, they can be written:

$$d(S_1, S_2) = \| \log(S_1) - \log(S_2) \|. \tag{2}$$

**Boundary Problems and Symmetry Principle**   Contrary to the classical Euclidean framework on tensors, one can clearly see from Eq. (2) that matrices with null or negative eigenvalues are at an infinite distance from tensors and will not appear in practical computations.

Moreover, distances are not changed by inversion, i.e. the *symmetry principle* is verified. As a consequence, the Log-Euclidean mean between tensors will be a generalization of the *geometric mean* and not of the arithmetic mean as in the classical Euclidean case. This is crucial for instance for a correct interpolation of determinants when two tensors are interpolated.

**Invariance by Similarity**   Among all Log-Euclidean metrics on the tensor space, some are invariant by similarity (rotation plus scaling). This means that if tensors are covariance matrices, computations on tensors using such a metric will be invariant with respect to a change of coordinates obtained by a similarity. A similarity-invariant Log-Euclidean metric (maybe the simplest one!) is given by:

$$d(S_1, S_2) = \left( \text{Trace} \left( \{ \log(S_1) - \log(S_2) \}^2 \right) \right)^{\frac{1}{2}}. \tag{3}$$

**Euclidean Calculus in the Logarithmic Domain**   The tensor vector space with a Log-Euclidean metric is in fact isomorphic and *isometric* with the corresponding Euclidean space of symmetric matrices. As a consequence, the Riemannian framework for statistics and analysis is extremely simplified, much simpler than in [10, 14, 15]. In particular, the Log-Euclidean mean of $N$ tensors is given by:

$$\mathbb{E}_{LE}(S_1, ..., S_N) = \exp \left( \frac{1}{N} \sum_{i=1}^{N} \log(S_i) \right). \tag{4}$$

*This is remarkable: in this framework, the interpolation, extrapolation, anisotropic diffusion, etc. of tensors can simply be performed in a Euclidean way in the logarithm domain, and final*

*results are mapped back to the tensor domain with the exponential.* Hence, statistical tools or PDEs can be generalized to tensors very readily. Mathematical issues such as existence and uniqueness of such PDEs on tensors are simply particular cases of the classical PDE theory on vector fields [16]. This is a striking result since so far the theory of the existence and uniqueness of general PDEs on tensors is still an open research field [17].

**Comparison with Affine-Invariant Metrics**  As shown in [18] and in Section 5 of [9], Log-Euclidean computations provide results similar to their affine-invariant equivalent, presented in [8]. The reason is the two families of metrics provide two generalizations of the geometric mean of positive numbers on tensors. Contrary to the Log-Euclidean mean, there is in general no closed form for the affine-invariant mean but rather a *barycentric equation.* Nevertheless, the determinants of the two means are both equal to the scalar geometric mean of the determinants of the averaged tensors [9]. This explains their likeness and the absence of swelling effect in both cases. This resemblance between the two means propagates to general computations which involve averaging, such as interpolation, extrapolation and regularization. The two means are even identical in a number of cases, in particular when averaged tensors commute. Yet they are *not* equal in general: Log-Euclidean means are slightly more anisotropic. As shown in [18], computations are *much* faster in the Log-Euclidean framework, by a factor of at least 4. They are also much simpler.

**Practical Use**  The use of Log-Euclidean metrics practically consists in taking the matrix logarithm of tensors, running computations on these vectors, and mapping the result back to the tensor space with the matrix exponential. In the next section, we apply this straightforward principle to the resolution of the joint estimation and smoothing of clinical DTI.

## 3   Joint Estimation and Regularization of Clinical DTI

The joint estimation and regularization of DTI can be handled in a variational formulation, i.e. one has to minimize the following energy functional:

$$E(D) = \frac{1}{2}\text{Sim}(D) + \frac{\lambda}{2}\text{Reg}(D) \tag{5}$$

with $\text{Sim}(.)$ being the data attachment term (estimation) and $\text{Reg}(.)$ being the regularization term. $\lambda$ is a factor of normalization between the two terms. In the following, we first present the estimation term, then the regularization term.

### 3.1   A Least Square Criterion on the Original DWI Intensities

As mentioned in Sec. 1.1, our noise model leads us to estimate directly the tensor field from the images and not their logarithm versions. One has to find the tensor field that

minimizes the energy functional [5]: $\sum_{i=1}^{N} \int_{\Omega} (\hat{S}_i - S_i)^2$. To fully benefit from the Log-Euclidean framework (Sec. 2), i.e. to carry on computations on a vector space, one simply parameterizes the tensor $D$ by its logarithm $L$ so that $D = \exp(L)$:

$$\mathrm{Sim}(L) = \sum_{i=1}^{N} \int_{\Omega} (\hat{S}_i - S_0 \exp(-bg_i^T \exp(L)g_i))^2.$$

After differentiation, one obtains:

$$\nabla\mathrm{Sim}(L) = 2b \sum_{i=1}^{N} \left( \hat{S}_i - S_i \right) S_i \left( \partial_{G_i} \exp(L) \right). \tag{6}$$

with $G_i = g_i g_i^T$ and $N$ the number of encoding gradients. In the last formula, the directional derivatives of the exponential ($\partial_G \exp(L)$) appear. For general matrices, one has to compute the series $\partial_G \exp(L) = \sum_{k=1}^{+\infty} 1/k! \sum_{i=0}^{k-1} L^i G L^{k-i-1}$ [9]. However, in the case of symmetric matrices, the differential is simplified. Let $L = R^T S R$ with $S = \mathrm{diag}(s_1, s_2, s_3)$. We have $\partial_G \exp(L) = R^T \partial_{RGR^T} \exp(S) R$. As $S$ is diagonal, one can access the $(l, m)$ coefficient of the resulting matrix as:

$$[\partial_{RGR^t} \exp(S)]_{l,m} = (\exp(s_l) - \exp(s_m))/(s_l - s_m) \left[ RGR^T \right]_{l,m}.$$

Finally, the minimization is achieved through a simple first order gradient descent: $L_{t+1} = L_t - dt \, \nabla\mathrm{Sim}(L_t)$. Thanks to the Log-Euclidean metric, $L$ belongs to a vector space and this evolution equation is actually a geodesic marching. After convergence, one simply needs to exponentiate the vector $L$ to obtain a tensor: $D = \exp(L)$.

## 3.2 An Anisotropic Regularization Term

The anisotropic regularization of the tensor field can be handled through the minimization of a $\phi$-functional: $\mathrm{Reg}(L) = \int_{\Omega} \phi \left( \|\nabla L\| \right)$. As we are working on a vector space, the gradient of this criterion can be expressed as follows, using $\psi(s) = \phi'(s)/s$:

$$\nabla\mathrm{Reg}(L) = -2\mathrm{div} \left( \psi \left( \|\nabla L\| \right) \nabla L \right) = -2\psi \left( \|\nabla L\| \right) \Delta L - 2 \sum_{i=1}^{3} \partial_i \left( \psi \left( \|\nabla L\| \right) \right) \partial_i L. \tag{7}$$

The key for the numerical implementation is the computation of the matrix and scalar fields $\partial_i L$, $\Delta L$ and $\|\nabla L\|$ of $\mathbb{R}^3$. Using a finite difference scheme, these are simply: $\partial_i L(x) = (L(x + x_i) - L(x - x_i))/(2\|x_i\|)$, $\Delta L(x) = \sum_{i=1}^{3} (L(x + x_i) - 2L(x) + L(x - x_i))/\|x_i\|^2$, and $\|\nabla L(x)\|^2 = \sum_{i=1}^{3} \|\partial_i L(x)\|^2$ ($\|.\|$ being the norm of Sec. 2).

The $\phi$-function gives an anisotropic behavior to the regularization, i.e. it will preserve the edges of the tensor field while smoothing homogeneous regions. For the experiments, we

used $\phi(s) = 2(1 + s^2/\kappa^2)^{1/2} - 2$ and $\psi(s) = (1 + s^2/\kappa^2)^{-1/2}$ as in [7]. $\kappa$ can be seen as a normalization factor for the gradient.

Finally, by combining Eq. (6) and (7), one obtains the evolution equation which leads to the minimization of the criterion 5: $L_{t+1} = L_t - dt\nabla E(L_t) = L_t - dt/2\left(\nabla\mathrm{Sim}(L_t) + \lambda\nabla\mathrm{Reg}(L_t)\right)$. Of course, one has to take the exponential of the solution to obtain a tensor.

## 4 Results on Synthetic and Clinical Data

To illustrate the benefits of our method, we perform 3 types of estimation on synthetic and real data. First, we perform a classical estimation on the scalar logarithm of the images. Second, the estimation is done using the least square (LSQ) criteria on DTI intensities. Finally, the regularization term is added (LSQ + regularization). Results are presented and discussed in the following.

### 4.1 Synthetic Data

We synthetically generated a tensor field containing two regions with orthogonal anisotropic tensors (Fig. 2 a). The DWI are artificially created (Fig. 2 b) using the Stejskal-Tanner equation and 7 diffusion gradients simulating the real data below. Finally, a centered Gaussian noise is added (variance of 0.01) to each DWI. The parameters used for the estimation are: $\lambda = 1.0$ and $\kappa = 0.2$. Results of the 3 estimations are shown in Fig. 2 c,d and e.

In Fig. 2 c, some tensors are missing: these are actually non-positive matrices that are not displayed. With the LSQ on DTI intensities (Fig. 2 d), these outliers disappear. The regularization term (Fig. 2 e) smoothed the field while preserving the discontinuity between the homogeneous regions.

### 4.2 Clinical Data

We tested the methods on 2 clinical datasets of medium and low quality. First, we used a brain dataset (Fig. 3 and 4) acquired with 7 encoding gradients (Basser sequence [1]) and a b-value of 1000 s.mm$^{-2}$. The dimensions of the images are $128 \times 128 \times 30$ and the spatial resolution is $1.875 \times 1.875 \times 4\mathrm{mm}^3$. Second, we used an experimental acquisition of the spinal cord(Fig. 5 and 6), with the same 7 encoding gradients and b-value as previously. The dimensions are $128 \times 128 \times 24$ (acquisition is coronal) with a spatial resolution of $1.4 \times 1.4 \times 1.4\mathrm{mm}^3$. This new type of acquisition will be generalized in a near future and is difficult to perform. Indeed, the patient often cannot stay too long in the scanner due to the pathology. Moreover, the small entrance of the scanner obliges the patient to have an uncomfortable position, and the scanning time must be shortened. Finally, the coil cannot be perfectly adapted to the body as it is for the head. The images are consequently much noisier than for the brain MRI. The parameters used for the processing are: $\lambda = 2.0, \kappa = 0.1$ for the brain dataset and $\lambda = 1.0, \kappa = 0.1$ for the spinal cord.
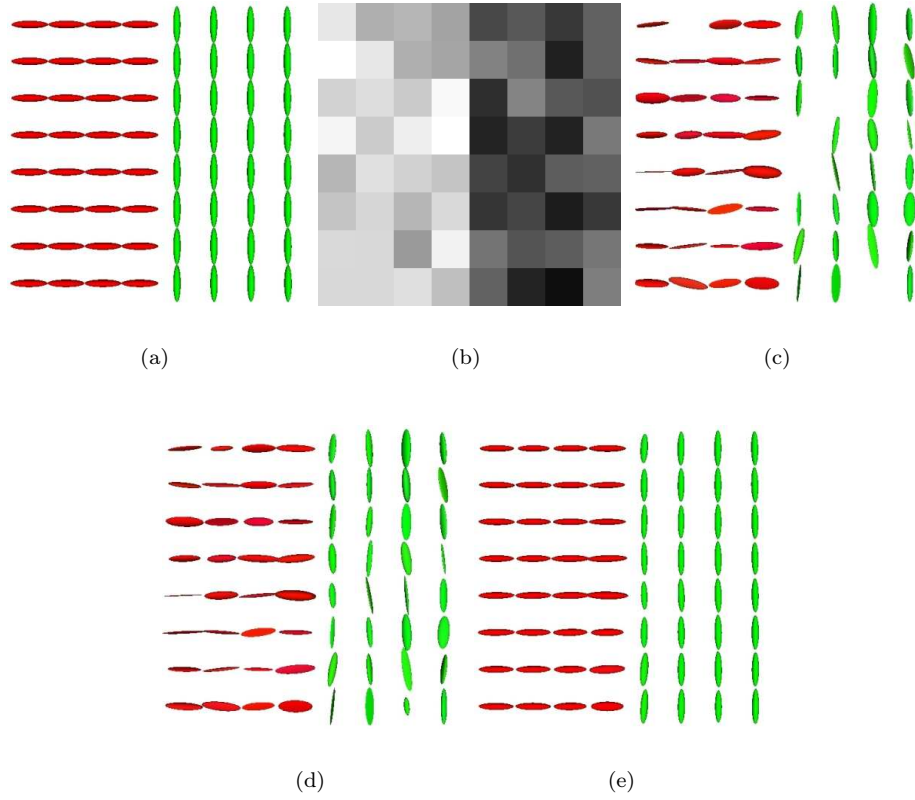
Figure 2: **Estimation of the tensor field from the noisy synthetic data. (a):** a 2D slice of the 3D synthetic field. **(b):** a 2D slice of a synthetic DWI (gradient: (0,1,0)) + noise, **(c):** the classical estimation, **(d):** the LSQ on DTI intensities, **(e):** the LSQ + regularization.

Fig. 3 and 5 show the fractional anisotropy (FA) (top row) for the three estimations and a close-up on the tensor field (bottom row). We see in both cases (Fig. 3 and 5 left) that the classical estimation introduces non-positive matrices ("holes" in the tensor field). The LSQ on DTI intensities (Fig. 3 and 5 middle) corrected these missing values. Finally, the LSQ plus the regularization smoothed the tensors and preserved the boundaries between the ventricles and the nearby tract (splenium) (Fig. 3 right), and between the spinal cord and nearby structures (Fig. 5 right). The FA is also regularized and transitions between isotropic (dark regions) and anisotropic (bright regions) tensors are preserved. We now exemplify this last point with the fiber tracking of the two datasets.
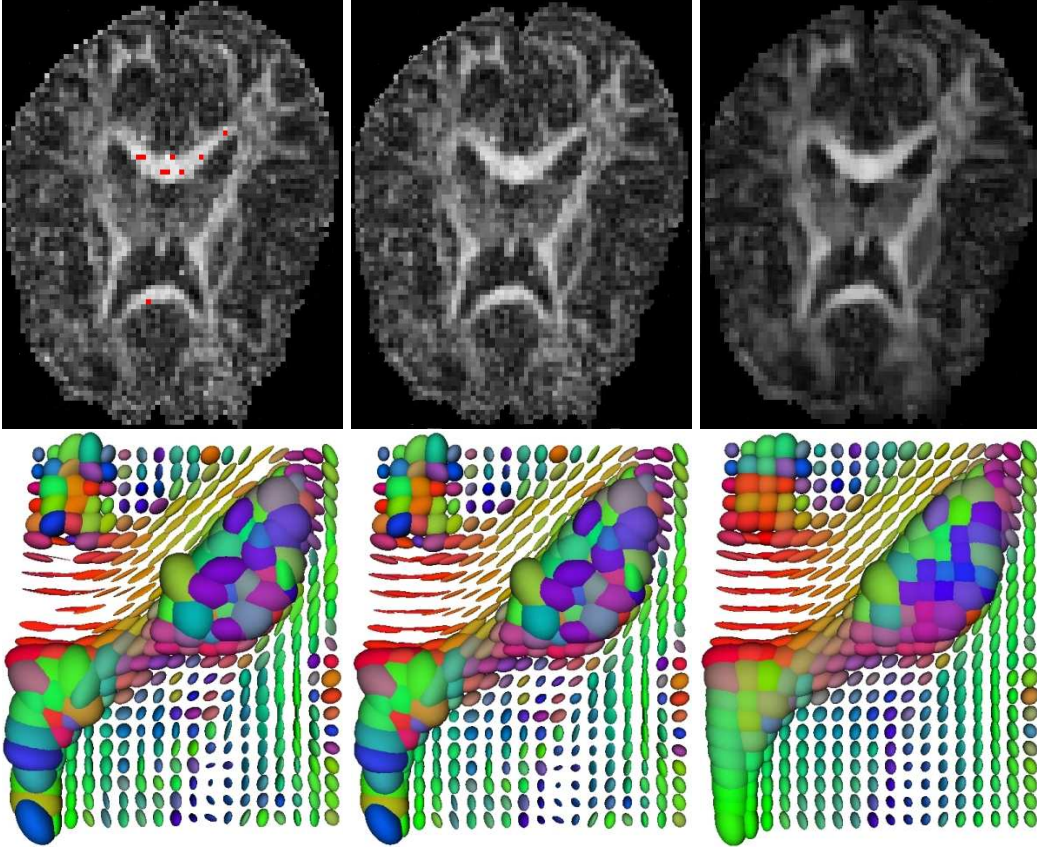
Figure 3: **Estimation of brain DTI and fiber tracking. Top row (3 first images):** fractional anisotropy. **Bottom row (3 first images):** a close-up on the top right ventricle and nearby. **From left to right:** classical estimation, LSQ on DTI intensities, LSQ + regularization. The color codes for the direction of the tensors: **red:** left-right, **green:** anterior-posterior, **blue:** inferior-superior. The red dots of the left image are voxels with non-positive tensors.

## 4.3  Improvement of Tractography

At the very end of the DTI processing pipeline resides the tractography, or fiber tracking. Among the numerous available methods for tracking fibers, we chose a relatively fast and easy to implement method [19] and show how the tracking can be improved by our variational estimation combined with regularization. Prior to the tracking, tensor fields are resampled so that the voxels are isotropic: in general, the out-plane resolution is very low (this is the case of the brain dataset here) and interpolating the tensors improves the regularity of the fibers. Resampling is interpreted as a weighted mean with trilinear coefficients. Such a mean
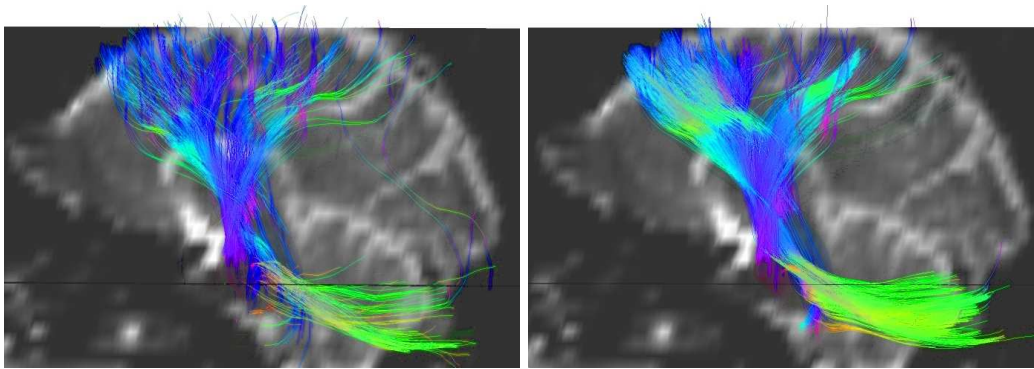
Figure 4: **Improvement of fiber reconstruction Left:** The corticospinal tract reconstructed after a classical estimation. **Right** The same tract after the joint estimation and smoothing proposed here.

is computed in the logarithmic domain and then mapped back to the tensor space with the matrix exponential: $D = \exp(\sum_{i=1}^{N} \omega_i \log(D_i))$.

We tracked the fibers from the tensor fields obtained after a classical estimation plus resampling and our estimation plus resampling. Results of tracking in the brain and the spinal cord are shown in Fig. 3 and 5 (top and bottom right images). With our estimation, the tracking is qualitatively much smoother in both cases and shows less dispersion. The overall number of fibers reconstructed is also greater. The smoothness of the tensor field indeed leads to more regular and longer fibers: tracts that were stopped due to the noise are now fully reconstructed. However, a quantitative analysis of the influence of the method on the tracking would be necessary.

# 5 Conclusion

This paper presents a new methodology to process noisy DT-MRI typical of clinical applications through a joint estimation and regularization of the diffusion tensor field. In particular, the estimation, which assumes an additive noise, is done on the DWI intensities and the tensor field itself is regularized. To optimize the criterion, we use a Log-Euclidean metric that has the advantage to provide a fast and easy to use framework to process tensors and to completely overcome the limitations of the standard Euclidean calculus. We successfully applied the method on two clinical datasets (brain and spinal cord DTI). The promising improvement of the fiber reconstruction of these data shows that even clinical MRI can be used for tractography.

In the future, the LSQ criteria could be advantageously replaced by a M-estimator to further improve the robustness of the estimation. Finally, the impact on the tracking must

be quantified. We are currently working on developing a dispersion measure of the fibers for that purpose.

# References

[1] P. Basser, J. Mattiello, and D. Le Bihan. MR diffusion tensor spectroscopy and imaging. *Biophysical Journal*, 66:259–267, 1994.

[2] C.-F. Westin, S. Maier, H. Mamata, A. Nabavi, F. Jolesz, and R. Kikinis. Processing and visualization for diffusion tensor MRI. *Medical Image Analysis*, 6(2):93–108, 2002.

[3] R. Deriche, D. Tschumperlé, and C. Lenglet. Dt-mri estimation, regularization and fiber tractography. In *International Symposium on Biomedical Imaging*, pages 9–12, 2004.
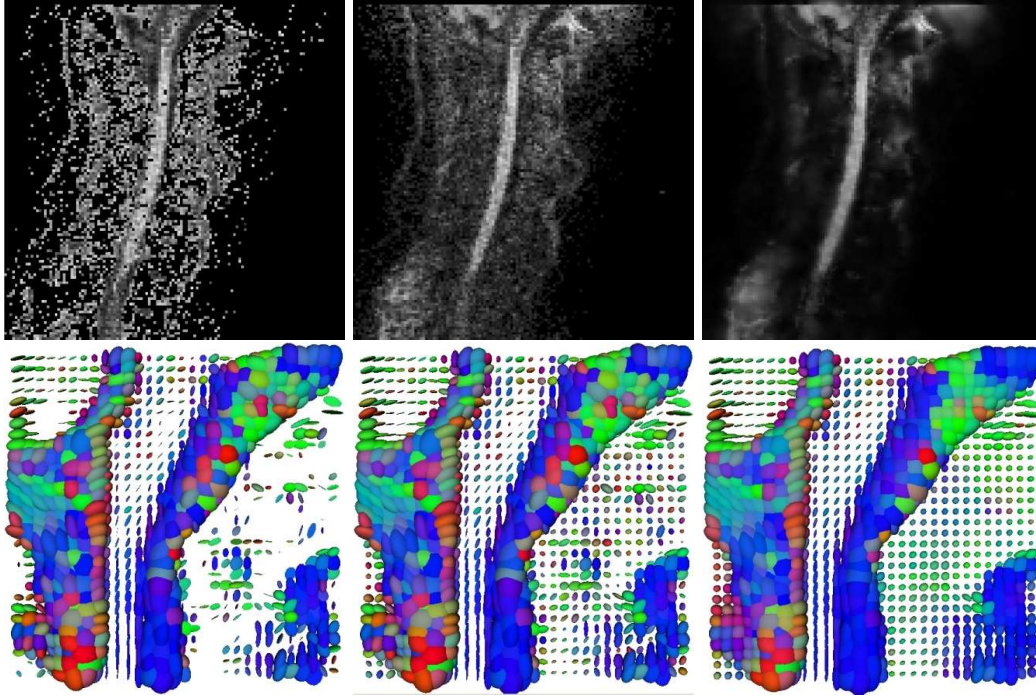
Figure 5: **Estimation of spinal cord DTI and fiber tracking. Top row (3 first images):** fractional anisotropy. **Bottom row (3 first images):** a close-up on the top the spinal cord and nearby. **From left to right:** classical estimation, LSQ on DTI intensities, LSQ + regularization.
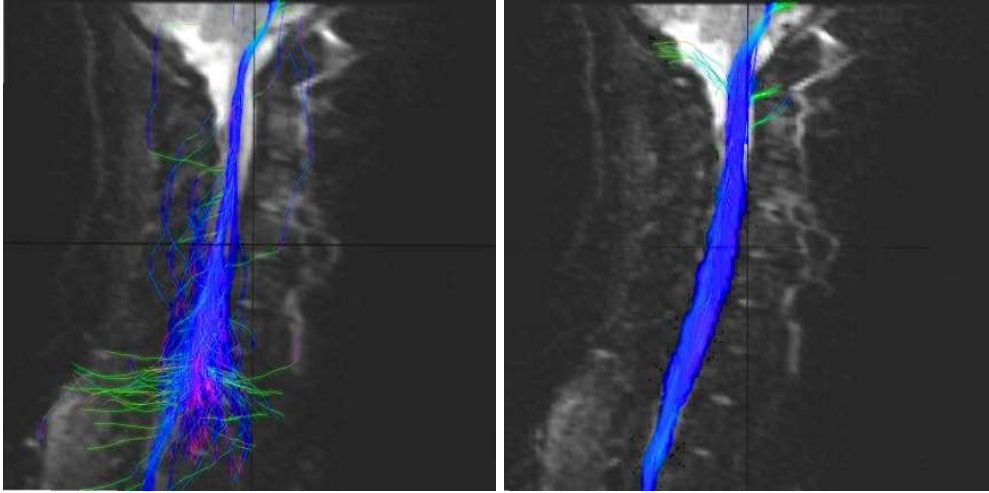
Figure 6: **Spinal cord fiber tract reconstruction. Left:** The spinal cord reconstructed after a classical estimation. **Right:** The same tract after our proposed variational framework.

[4] R. Salavador, A. Peña, D.K. Menon, T.A. Carpenter, J.D. Pickard, and E.T. Bullmore. Formal characterization and extension of the linearized diffusion tensor model. *Human Brain Mapping*, 24:144–155, 2005.

[5] Z. Wang, B.C. Vemuri, Y. Chen, and T.H. Mareci. A constrained variational principle for direct estimation and smoothing of the diffusion tensor field from complex DWI. *IEEE Transactions on Medical Imaging*, 23(8), August 2004.

[6] O. Coulon, D. Alexander, and S. Arridge. Diffusion tensor magnetic resonance image regularization. *Medical Image Analysis*, 8(1):47–67, 2004.

[7] C. Chefd'hotel, D. Tschumperlé, R. Deriche, and O. Faugeras. Constrained flows of matrix-valued functions: Application to diffusion tensor regularization. In *Proceedings of ECCV'02*, LNCS 2350, pages 251–265. Springer Verlag, 2002.

[8] Xavier Pennec, Pierre Fillard, and Nicholas Ayache. A Riemannian framework for tensor computing. *International Journal of Computer Vision*, 65(1), October 2005. Also as INRIA Research Report 5255.

[9] V. Arsigny, P. Fillard, X. Pennec, and N. Ayache. Fast and simple computations on tensors with Log-Euclidean metrics. Research Report RR-5584, INRIA, Sophia-Antipolis, France, May 2005.

[10] P. Fletcher and S. Joshi. Principal geodesic analysis on symmetric spaces: Statistics of diffusion tensors. In *Proceeding of CVAMIA and MMBIA*, LNCS 3117, pages 87–98, 2004.

[11] C. Lenglet, M. Rousson, R. Deriche, and O. Faugeras. Statistics on multivariate normal distributions: A geometric approach and its application to diffusion tensor MRI. Research Report 5242, INRIA, 2004.

[12] P. Batchelor, M. Moakher, D. Atkinson, F. Calamante, and A. Connelly. A rigorous framework for diffusion tensor calculus. *Magnetic Resonance in Medecine*, 53:221–225, 2005.

[13] Xavier Pennec. Probabilities and Statistics on Riemannian Manifolds: A Geometric approach. Research Report 5093, INRIA, January 2004. submitted to Int. Journal of Mathematical Imaging and Vision.

[14] C. Lenglet, M. Rousson, R. Deriche, and O. Faugeras. Statistics on multivariate normal distributions: A geometric approach and its application to diffusion tensor MRI. Research Report 5242, INRIA, June 2004.

[15] M. Moakher. A differential geometry approach to the geometric mean of symmetric positive-definite matrices. *SIAM Journal on Matrix Analysis and Applications*, 2004. To appear.

[16] G. Sapiro. *Geometric Partial Differential Equations and Image Analysis*. Cambridge University Press, Cambridge, UK, 2001.

[17] C. Chefd'hotel, D. Tschumperlé, R. Deriche, and O. Faugeras. Regularizing flows for constrained matrix-valued images. *Journal of Mathematical Imaging and Vision*, 20(1-2):147–162, 2004.

[18] Vincent Arsigny, Pierre Fillard, Xavier Pennec, and Nicholas Ayache. Fast and simple calculus on tensors in the Log-Euclidean framework. In *Proceedings of MICCAI'05*, LNCS, Palm Springs, California, October 2005. Springer Verlag. To Appear.

[19] P. Fillard and G. Gerig. Analysis tool for diffusion tensor MRI. In *Proceedings of MICCAI'03*, number 2 in LNCS 2878, pages 967–968, 2003.